IET Science, Measurement & Technology

DOI: 10.1049/smt2.12060

The Institution of Engineering and Technology WILEY

ORIGINAL RESEARCH PAPER

A general method for radiated emission prediction in a multiple monopole source stirred reverberation chamber

Alfredo De Leo | **Graziano Cerri** | **Paola Russo** | **Valter Mariani Primiani**

Department of Information Engineering, Università Politecnica delle Marche, Ancona, Italy

Correspondence
Alfredo De Leo, Department of Information Engineering, Università Politecnica delle Marche, Via B. Bianche 12, Ancona, Italy.
Email: a.deleo@univpm.it

Abstract

This paper presents a general and quasi-analytical method aimed at reconstructing the electric field radiated by equipment under test (EUT), in free space through the knowledge of the values of the electric field sampled on the walls of a rectangular metallic enclosure. The algorithm is based on a set of equivalent magnetic and electric currents, regularly placed in a sub volume of the chamber, whose values are determined to reconstruct the electric field due to the EUT on the samples. Results show that the method is general because it can be applied to a wide set of EUTs, but it is also flexible because it is able to exploit some *a priori* knowledge of the source to improve its accuracy and efficiency.

1 | INTRODUCTION

Reverberation chambers (RCs) are used in electromagnetic compatibility for immunity and emission tests. In particular, the measurement of power radiated by equipment under test (EUT) inside an RC has been studied since 1976 [1].

Inside a well operating RC, the electromagnetic field is statistically uniform and isotropic, thus so making the EUT directivity meaningless [2,3]. Therefore, radiated emission measurements in an RC [4] are based on the estimation of the equivalent directivity (D) of the EUT as a function of its geometry [5,6].

In 2013, a new method, based on the Rician K factor, for estimating the directivity of radiating devices in a reverberation chamber was proposed [7]. One year later, using an improvement of this technique, an antenna radiation pattern was obtained by performing only one measurement per angle under study, taking advantage of the real-time Doppler effect [8], therefore making radiation pattern retrieval very competitive compared to traditional anechoic chamber methods.

In 2016, a free space antenna radiation pattern estimation from intensity measurements made in reverberating environments was investigated [9], examining, in particular, the scenario where the field statistics deviate from the ideal ones.

In the literature, many research activities were also addressed for predicting the emissions of an EUT located in an open area test site (OATS) from measurement done in other environments. In addition to the correlation with free space measurement [10], typically reproducible in a fully anechoic chamber, these activities also aim at formulating a set of equivalent sources able to replace the EUT in computing its radiation.

As regards measurement sites alternative to OATS in conjunction with the use of equivalent sources, transverse electromagnetic (TEM) cells were first investigated. In particular, an electrically small radiating source of arbitrary nature placed into a TEM cell was modelled by an equivalent-dipole system consisting of three orthogonal electric dipoles and three orthogonal magnetic dipoles, each excited with arbitrary amplitude and phase [11].

In [12], the author reviews the basics of the multipole model as it relates to TEM cells, details various measurement schemes appropriate to single-port TEM cells, and presents examples of measured emission data, both in near field and in far field.

A review of dipole models for correlating measurements made in various electromagnetic compatibility test facilities was presented in [13]: a fully anechoic chamber, an open area test site (OATS) or a semi-anechoic chamber (SAC), a transverse electromagnetic (TEM) cell or stripline, and a reverberation chamber.

GTEM cell measurements of an EUT were also proposed for predicting the equivalent OATS radiated field [14,15]. The EUT is modelled by equivalent sources and the algorithms used are based on several *a priori* assumptions on amplitude, phase and position of the multipoles and their influence on the simulated OATS field.

Successively, the paper [16] presented a time-domain transmission line to model the GTEM cell. The advantages of this method include high accuracy and the ability to model different materials. The model of a realistic EUT was also included in the GTEM characterization and a good agreement between the experimental measurement of radiated emissions and simulations was obtained.

Later, in [17] the procedure to convert total radiated power measurements data to equivalent electrical field data, which might be obtained on a standardized test site, was discussed. The proposed algorithm is based on two parameters, the geometrical factor and the directivity of the equipment under test. Both parameters are unknown for unintentional radiators, and, in particular, the directivity depends on the effective size of the EUT, described by the radius of a sphere containing it.

More recently, in [18] an improvement for the standard algorithms used to correlate the radiated emission measurements performed in a GTEM cell to measurements performed in an OATS was proposed. The improvement was achieved by using non-linear regression models in order to estimate the amplitudes of a multipole model, assuming equally phased dipole moments.

The analysis of the literature shows how the correlation among measurements carried out in different test sites is of great importance in EMC, from both a standardization viewpoint [19] and a scientific one [20].

This paper proposes a model for estimating the radiated emissions of an EUT in free space from the knowledge of the field radiated by the EUT in a closed environment. The model development is still at a theoretical level, necessary for the analysis of all the parameters that can affect its accuracy. More specifically, the main goal of the paper is to apply the idea to an EUT inside an RC. In particular, the method appears to be very suitable for RCs that implement the multiple monopole source stirring (MMSS) technique [21,22], due to the presence of arrays of monopoles on the RC's walls for the stirring action, and useful, in the emission test, for sampling the electric field.

The proposed method consists in the determination of a set of elementary equivalent electric and magnetic sources, placed into a sub volume called equivalent source volume (ESV), and fed with currents able to generate the same electric field values of the EUT in the RC. Subsequently, the equivalent sources are placed in free space, under the assumption that their radiated field is the same field radiated by the EUT in free space. To check the validity of the proposed method, that is, the equivalence between the elementary sources and the EUT also in free space, some EUTs, whose radiation can be analytically determined, have been tested.

It is important to specify that the term 'equivalent source' is not used in the sense described by the equivalence principle, rather, throughout the paper, the term is simply used with the meaning of 'good approximation' of the reference sources.

The organization of the paper is as follows: Section 1 describes the method and the scenario; Section 2 reports results to validate the method; Section 3 shows that by using a subset of equivalent sources, results can be further improved and, finally conclusions and future works are reported.

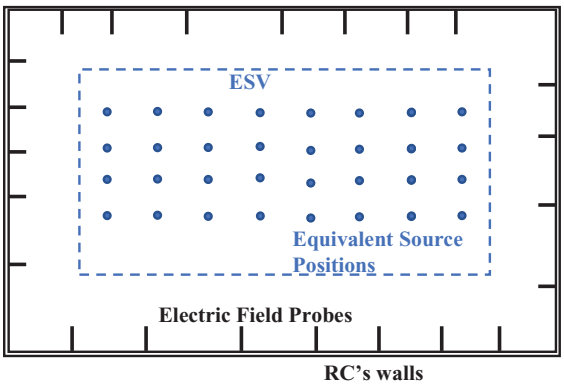

FIGURE 1 Electric field probes on the chamber walls (black) and the ESV containing the grid of equivalent sources (blue)

2 | DESCRIPTION OF THE METHOD

The scenario (Figure 1) consists in a rectangular cavity with metallic walls, whose conductivity is chosen to take into account all lossy mechanisms. An EUT is placed into the equivalent source volume (ESV), usually close to the centre, even though this allocation is not critical for the method application. N_s electric field samples are collected on the RC walls. The aim of this section is to investigate theoretically if it is possible to estimate, with acceptable accuracy, the radiated emissions of the EUT in free space, from the knowledge of the electric field in a certain number of sampling points collected on the walls of the RC. The proposed method requires the definition of equivalent sources that can represent the EUT emissions both in the RC and in free space.

The model is based on the assumption that the emission of the EUT does not appreciably change when passing from the RC environment to free space. This assumption is acceptable if we consider the EUT within a well operating RC. It is worth specifying that the method was designed as an application of the MMSS-RC, because the chamber is characterized by many antennas on the chamber walls, therefore, the electric field can be easily sampled. However, the method can be generalized using a set of electric field probes in a generic rectangular cavity.

The main goal is to characterize the EUT (the reference scenario) with a set of elementary sources, electric and magnetic currents (the equivalent scenario or the equivalent sources), whose electromagnetic behaviour inside the MMSS RC can be analytically predicted [21].

The equivalent sources are uniformly placed in the sub volume ESV of the RC. Three electric and three magnetic dipoles, having orthogonal directions, are placed in each node of a regular grid (Figure 1).

The amplitude and phase of equivalent sources are calculated considering that the electric field values sampled by the monopoles on the walls have to be the same for the reference and the equivalent scenario. The value of the current flowing in each equivalent elementary source is calculated according to the flow chart shown in Figure 2.

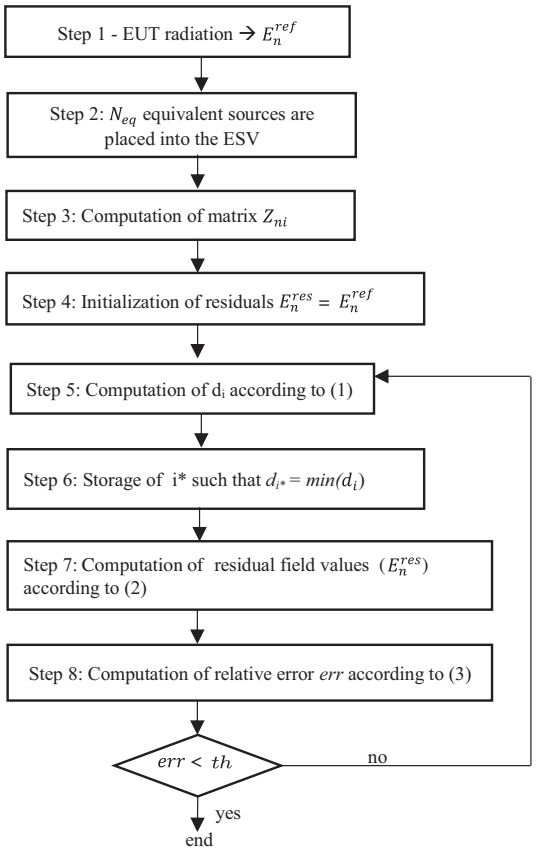

FIGURE 2 Flow chart of the proposed method

In the following, the algorithm operations pertaining to each step of the method are described:

- Step 1: the reference electric field radiated by the EUT (E_n^{ref}, n = 1, ..., Ns) is calculated in correspondence of the N_s sample points placed on the chamber's walls.
- Step 2: the EUT is removed and is substituted by a set of equivalent sources ($\vec{J}_i^{eq}, \vec{M}_i^{eq}$, $i = 1, \ldots, N_{eq}$) placed into the ESV. Their values are initially set to zero. The algorithm provides the final values of the equivalent sources with the desired accuracy at the end of the iterative procedure. The choice of the value of N_{eq} will be investigated in Section 2.
- Step 3: computation of the matrix Z_{ni}, being $n = 1, \ldots, N_s$ and $i = 1, \ldots, N_{eq}$; each element of the matrix represents the electric field generated by the ith equivalent source and normalized to the current, calculated at nth sample point.
- Step 4: the reference field (E_n^{ref}) is stored as the residual value (E_n^{res}).
- Step 5: the quantity d_i, defined as (1) is calculated for each ith equivalent source

$$d_i = \frac{\sum_{n=1}^{N_s} |E_n^{res} - Z_{ni} I_i|}{\sum_{n=1}^{Ns} \left|E_n^{ref}\right|}, \quad i = 1, \ldots, N_{eq} \tag{1}$$

(*Rev* 2.9, *Rev*. 2.13)

This quantity represents the error made in evaluating the field for each equivalent source.

- Step 6: the minimum value of d_i is chosen and the corresponding i*th equivalent source I_{i*} is fixed, because its field represents the best fitting of the EUT field.
- Step 7: (E_n^{res}) values of the electric field are updated by subtracting the electric field values generated by I_{i*} (2), obtaining a residual field.

$$E_n^{res} = E_n^{res} - Z_{ni*} I_{i*}, \; n = 1, \ldots, N_s \tag{2}$$

- Step 8: the relative error is computed according to (3).

$$err = \frac{\sum_{n=1}^{N_s} |E_n^{res}|}{\sum_{n=1}^{N_s} \left|E_n^{ref}\right|}. \tag{3}$$

If it assumes a value lower than a desired threshold (*th*) the algorithm ends, otherwise the procedure reiterates from Step 5, using the residual field as the new field to be reproduced by the equivalent sources. According to our experience, a value th ≤ 0.01 assures a good level of reliability of the algorithm.

At the end of the iterations, the algorithm provides a set of N_{eq} current values of elementary sources that generate on the RC walls the best approximation of the reference EUT field, and we assume that they also radiate in free space the same field of the EUT in free space, as shown in the next sections.

3 | RESULTS

The simulations reported in this section aim to demonstrate the capability of the proposed model to predict the radiation of an EUT in free space.

In the proposed technique, the equivalent source spatial distribution is a key point for its accuracy. Consequently, to analyze the effect of this parameter, the initial choice is to space the grid nodes at half a wavelength [23], then, this distance is varied to investigate any critical issues.

The scenario is an RC having dimensions of 80 cm × 90 cm × 100 cm, and the investigated frequency range is 1–6 GHz. The electric field is sampled in $Ns = 120$ points, irregularly placed onto the RC's walls. In the analytical model of this chamber, all loss mechanisms are taken into account in terms of an equivalent finite conductibility of the walls [21]. More details on the RC characterization, including quality factor, working frequencies, the well stirred conditions and the performances of the multiple monopole source stirring technique can be found in [24–26].

The EUT (Figure 3) consists in three dipoles and three square loops with orthogonal directions. This choice is due to two reasons: (1) the EUT radiation, both inside the RC and in free space, can be analytically calculated; (2) the source structure is quite general.

The EUT can be included in a cube with 30 cm sides. All the dipoles have a length of 1 cm and they are fed by a current of 0.1 A. All the loops have a side of 10 cm and their feeding current is

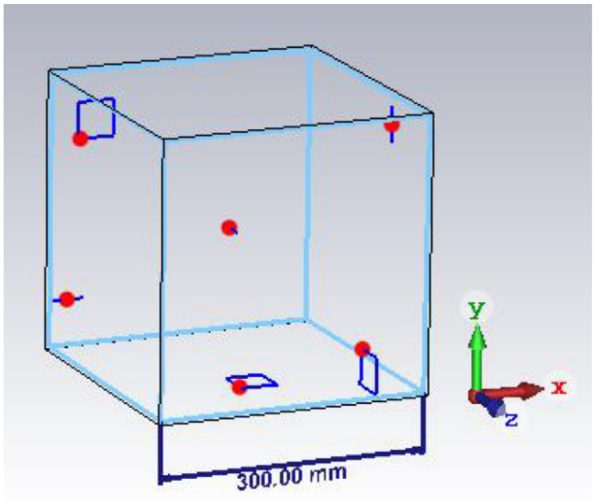

FIGURE 3 The EUT: Three dipoles and three loops having orthogonal directions in a cube with 30 cm sides

0.01 A. In this way, the electric field values on the sample points due to the loops have the same order of magnitude as those of the dipoles.

Considering, for example, a dipole of length l_d oriented along the z axis, placed in (x_d, y_d, z_d) and fed by a current $I_{\tilde{z}}$, the electric field orthogonal to the RC wall located on the RC side $x = 0$ is

$$E_x(y,z) = -\frac{16 I_{\tilde{z}}}{j\omega\varepsilon} \sum_{m,n,p} \left[\frac{1}{abd} \sin\left(k_y y\right) \sin\left(k_{\tilde{z}} z\right) \cdot \right.$$
$$\cdot \sin\left(k_{\tilde{z}} l_d\right) \sin\left(k_x x_d\right) \sin\left(k_y y_d\right) \sin\left(k_{\tilde{z}} z_d\right) \cdot \quad (4)$$
$$\left. \cdot \left(\frac{k_x}{k_{nmp}^2} + \frac{k_x k^2}{\delta_p k_{nmp}^2 \left(k_{nmp}^2 - k_{TM}^2\right)} \right) \right],$$

where

$$k_x = \frac{m\pi}{a}, \quad k_y = \frac{n\pi}{b}, \quad k_{\tilde{z}} = \frac{p\pi}{d},$$

$$k_{mnp}^2 = k_x^2 + k_y^2 + k_{\tilde{z}}^2, \quad k_c^2 = k_x^2 + k_y^2,$$

$$\delta_i = \begin{cases} 2, & i = 0 \\ 1, & i \neq 0 \end{cases},$$

$$k_{TE,TM}^2 = k^2 \left(1 - (j-1) \frac{\omega_{mnp}}{\omega\, Q_{mnp}^{TE,TM}} \right),$$

and k is the wavenumber, ω_{mnp} is the angular resonant frequency for the (m, n, p)th mode and $Q_{mnp}^{TE,TM}$ is the quality factor of the RC related to the (m, n, p)th TE or TM mode. This expression was derived in [21] starting from the general expression of a cavity field in terms of modal expansion [27].

Equation (4) is also an extended and specific representation of the general term $Z_{ni} I_i$ appearing in (1). Similar expressions

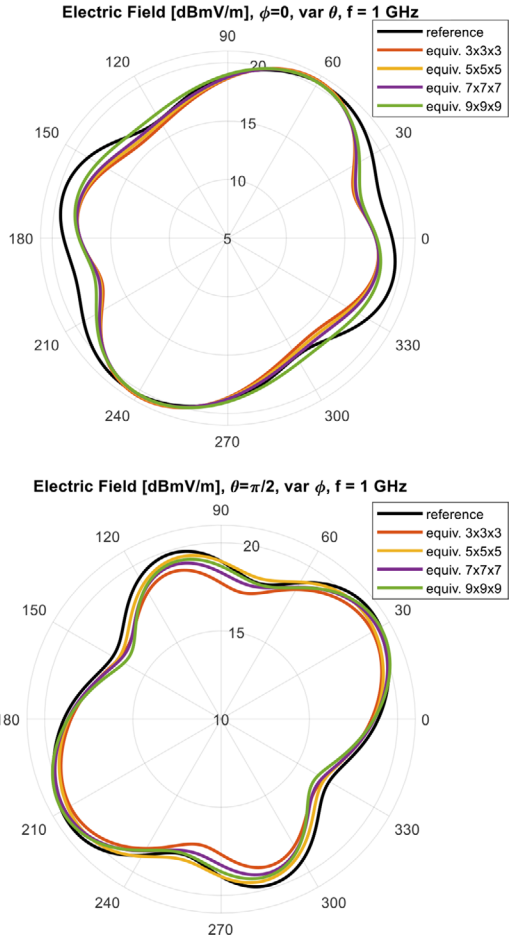

FIGURE 4 Polar plots of the reference and equivalent electric field, varying the number of equivalent sources at 1 GHz

can be derived for the electric field generated by all the other equivalent sources. Regarding the loops, they are modelled as a combination of four dipoles along the sides of a square.

We considered at first the frequency of 1 GHz, and we fixed the number of equivalent sources to 27, corresponding to a grid of 3 × 3 × 3 equivalent sources spaced half a wavelength apart. Then, we increased the number of equivalent sources to analyze the effect of reducing their relative distance.

Figure 4 reports the electric field intensity radiated in free space at a distance of 10 m in two orthogonal planes, reconstructed with our method and compared with the reference field. Emission patterns are evaluated varying the number of equivalent sources in the ESV. The figure shows that when the spacing between the equivalent sources is reduced, but their number is increased to maintain the same volume, there are no significant changes of the results.

Table 1 shows the effect of the equivalent source spacing on the directivity and on the maximum radiated field values. Δ_λ represents the distance between two adjacent equivalent sources in terms of wavelength, D_{ref} the reference directivity, D_{eq} the directivity due to the equivalent source reconstruction and $E_{\text{eq}}/E_{\text{ref}}$ the ratio between the maximum values of the equivalent electric field in free space and the reference value. For

TABLE 1 Effects of the equivalent sources spacing at 1 GHz

N_{eq}	Δ_λ	D_{ref}(dBi)	D_{eq}(dBi)	E_{eq}/E_{ref}(dB)	D_{est}(dBi)
3^3	1/2	2.3	2.7	0.01	3.7
5^3	1/4	2.3	2.6	−0.35	3.7
7^3	1/6	2.3	2.8	0.01	3.7
9^3	1/8	2.3	2.2	−0.39	3.7

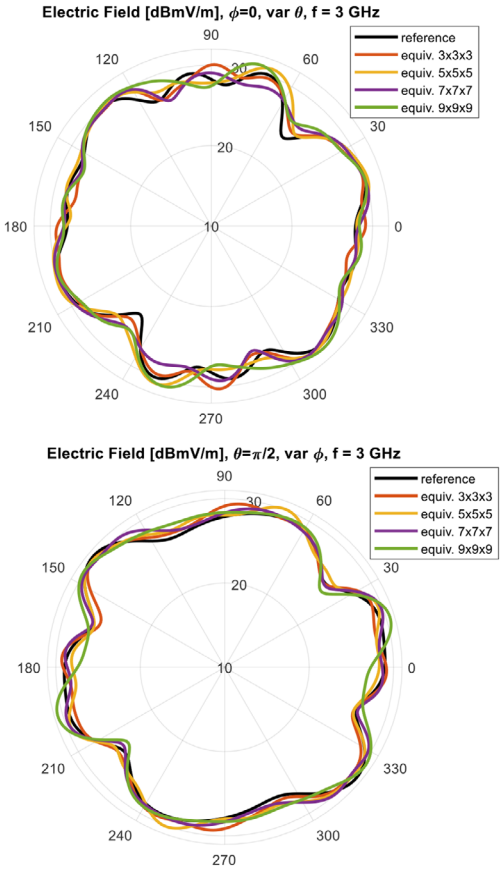

FIGURE 5 Polar plots of the reference and equivalent electric field, varying the number of equivalent sources at 3 GHz

the sake of comparison, D_{est} the directivity estimates according to the standard [4], is also reported.

To explore all the frequency ranges, we simulate the same scenario at the frequency of 3 GHz and 6 GHz and the results are reported in Figure 5 and Table 2, and in Figure 6 and Table 3, respectively.

TABLE 2 Effects of the equivalent sources spacing at 3 GHz

N_{eq}	Δ_λ	D_{ref}(dBi)	D_{eq}(dBi)	E_{eq}/E_{ref}(dB)	D_{est}(dBi)
3^3	3/2	2.8	2.8	0.10	5.2
5^3	3/4	2.8	2.6	−0.20	5.2
7^3	1/2	2.8	2.9	0.17	5.2
9^3	3/8	2.8	3.0	0.35	5.2

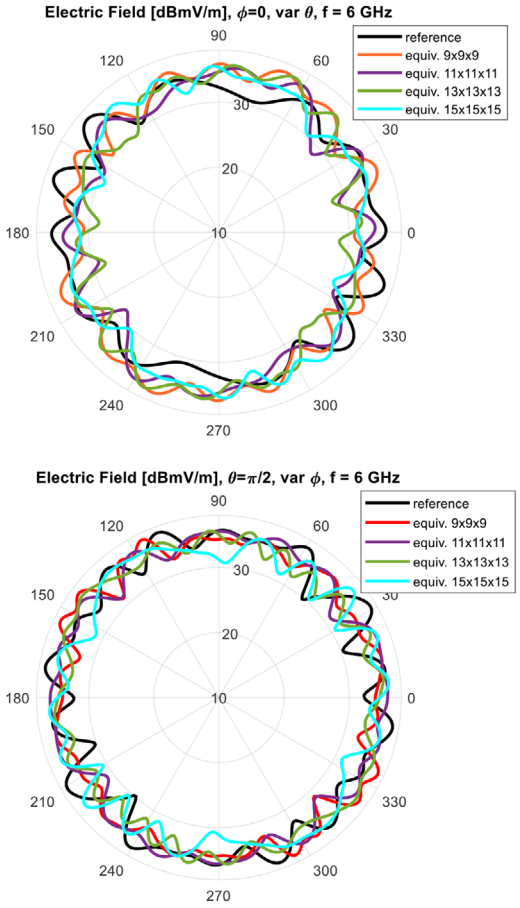

FIGURE 6 Polar plots of the reference and equivalent electric field, varying the number of equivalent sources at 6 GHz

TABLE 3 Effects of the equivalent sources spacing at 6 GHz

N_{eq}	Δ_λ	D_{ref}(dBi)	D_{eq}(dBi)	E_{eq}/E_{ref}(dB)	D_{est}(dBi)
9^3	3/4	3.8	3.5	1.71	6.3
11^3	3/5	3.8	4.4	1.03	6.3
13^3	1/2	3.8	4.2	1.36	6.3
15^3	3/7	3.8	3.7	1.31	6.3

From the previous results it can observed that, as expected, the half-wave spacing of the equivalent sources is a good choice for assuring efficiency and accuracy.

In the low frequency range, the equivalent sources are able to reconstruct with significant accuracy, all the investigated parameters, emission pattern, maximum emitted field intensity and directivity. In the higher frequency range, the emission pattern exhibits a highly oscillating behaviour, and this characteristic is well predicted by the model.

The maximum field value is also estimated with sufficient accuracy: at 1 and 3 GHz the error is smaller than 0.5 dB, and at 6 GHz the error is in the range [1,2] dB, however it provides a slightly overestimated value.

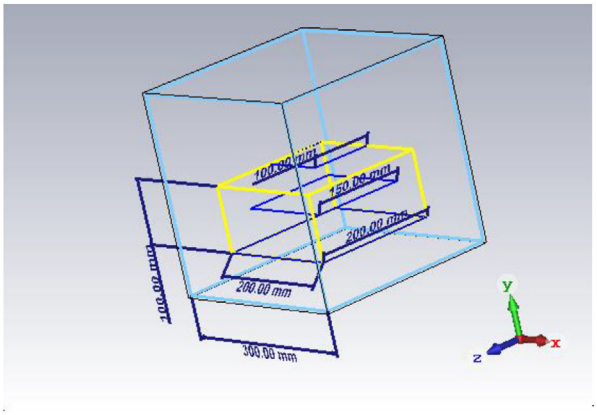

FIGURE 7 The EUT: Three parallel loops placed into a cube with 30 cm sides (light blue) and the volume containing them (yellow)

4 | USE OF A SUBSET OF EQUIVALENT SOURCES

In the previous section a completely general approach to model emission of an EUT in a cavity has been presented. The method is however very flexible, and one can use this characteristic to improve its efficiency and accuracy. In fact, all *a priori* knowledge of the EUT can be easily exploited in order to reduce the number of the equivalent sources required to represent the radiated field. For example, information concerning the EUT dimensions and shape, the presence of apertures or radiation critical points identified after visual inspection can be considered, taking advantage of a subset of the equivalent sources.

Three cases have been analyzed:

- the EUT consists in three parallel loops;
- the EUT has an aperture on a metallic chassis;
- the EUT has a cable protruding from a metallic chassis.

4.1 | Three parallel loops

We consider a generic EUT included in a cubic volume (30 cm × 30 cm × 30 cm), as shown in Figure 7. The EUT in the model is made of square loops, placed on three parallel planes spaced 5 cm apart and having the side lengths of 10 cm, 16 cm, and 20 cm, respectively. They represent three realistic circuits on PCBs mounted on a rack.

In this situation, we do not consider all equivalent sources as we have done in Section 2, but the algorithm automatically excludes all equivalent sources outside the volume occupied by the radiating elements of the EUT (20 cm × 20 cm × 10 cm). Figure 8 reports the electric field radiated in free space at the distance of 10 m at the frequency of 1 GHz.

Table 4 shows the effect of the equivalent source spacing in the sub volume occupied by the EUT on the directivity and on the maximum radiated field values. We can observe that the accuracy is comparable with that of the examples in Section 2, but the reduction of the equivalent sources used in the model is

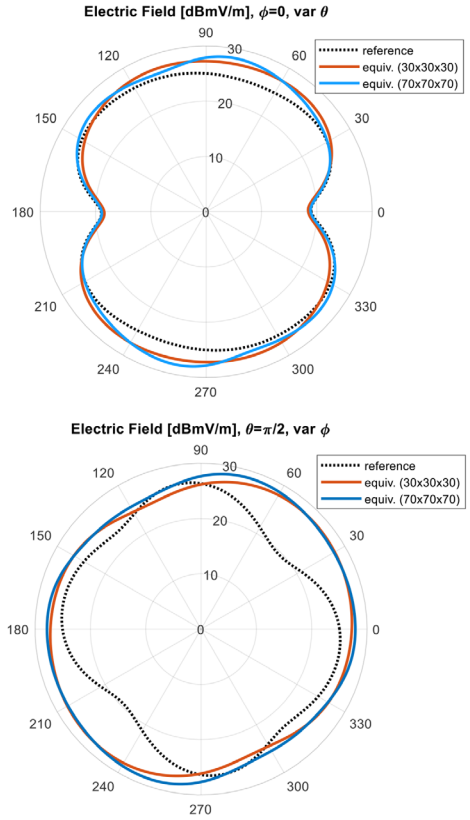

FIGURE 8 Reference and equivalent electric field radiated by three parallel loops at a distance of 10 m, at 1 GHz

TABLE 4 Model prediction—Scenario Figure 5

Eq. sourcesplacement	D_{ref}(dBi)	D_{eq}(dBi)	E_{eq}/E_{ref}(dB)	D_{est}(dBi)
Volume 30 × 30 × 30	3.1	2.8	0.49	3.7
Volume20 × 20 × 10	3.1	2.9	0.38	3.7
Volume70 × 50 × 60	3.1	2.7	0.52	3.7

78% (75 instead of 343 grid points), with a corresponding significant reduction of CPU time. Also, the accuracy of the predicted maximum values and emission pattern is slightly improved.

Table 4 also reports results for an ESV having dimensions of 70 cm × 50 cm × 60 cm, the largest dimension for the considered RC in order to maintain a distance of at least half a wavelength from the conducing walls. It is also noticeable that a great enlargement of the ESV does not provide a more accurate prediction of the radiated field. For the sake of brevity, emission patterns for this large ESV are not reported.

4.2 | EUT with an aperture on metallic chassis

The analysis reported in this section is a further example of a significant simplification of the 3D general model when *a priori* information can be used.

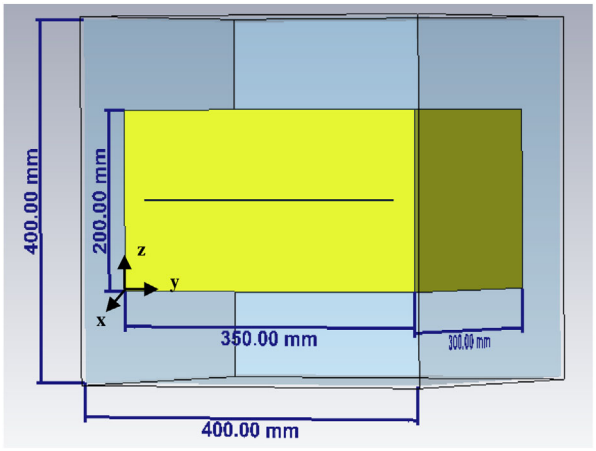

FIGURE 9 The EUT: A metallic box with a rectangular (300 mm × 1 mm) slot on one side

Let us assume we deal with the problem of an EUT having a metallic chassis with a rectangular aperture on one side. In this very common situation, it is evident that a simple visual inspection can identify the aperture as a possible source of electromagnetic emission.

In order to analyze a realistic and specific situation, we assume that the dimensions of the EUT are 20 cm × 35 cm × 30 cm; the slot is opened on the EUT side parallel to the y-z plane, and it has a length of $w = 30$ cm along the y-direction and a height $s = 1$ mm along the z-direction (Figure 9).

A TE_{10} distribution is assumed for aperture field $\vec{E}(y) = E_{ap}\cos(\pi y/w)\,\hat{z}$.

The assumed geometry allows us to analytically evaluate the reference field inside the chamber. As an example, the electric field on the RC wall $x = 0$, due to the aperture radiation is

$$E_x(y,z) = \frac{16\pi E_{ap}}{abdw}\sum_{m,n,p}\left[\frac{\cos(k_z z_{ap})\sin(k_y y_{ap})\cos(k_x x_{ap})}{k_y^2-\left(\frac{\pi}{w}\right)^2}\cdot\frac{\sin(k_z s)\cos(k_y w/2)\sin(k_y y)\sin(k_z z)}{k_c^2}\cdot\left(\frac{k_y^2}{\delta_m\delta_n\left(k_{nmp}^2-k_{TE}^2\right)}+\frac{k_{yx}^2}{\delta_p\left(k_{nmp}^2-k_{TM}^2\right)}\right)\right] \quad (5)$$

where x_{ap}, y_{ap} and z_{ap} are the coordinates of the aperture centre.

The reconstruction procedure is carried out at 1 GHz with a grid step of 5 cm, and comparing three equivalent source distributions:

- volumetric, choosing the equivalent sources corresponding the EUT's volume, with a grid of 280 points;
- superficial, choosing only the subset of the equivalent sources corresponding to the EUT's external surface [28]. In this case, the number of the grid points is 112;
- 'ad hoc', choosing only the subset of the equivalent sources corresponding to the slot. In this situation, the number of grid points is 7.

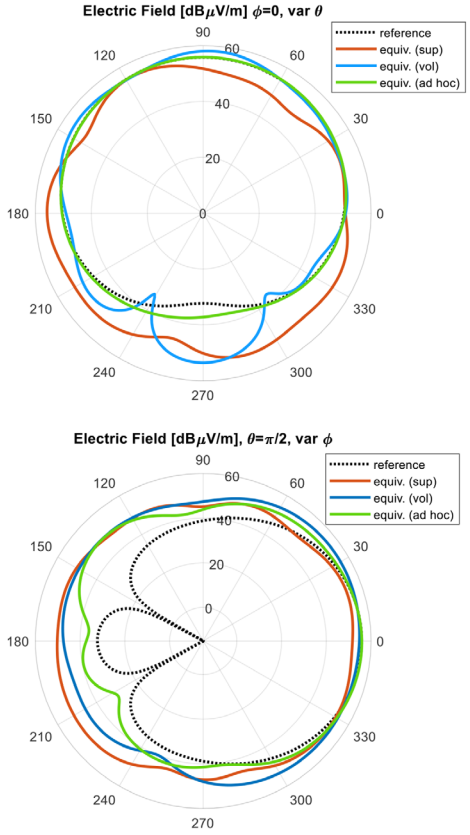

FIGURE 10 Electric field at the distance of 10 m radiated by an EUT having a 30 cm slot over a metallic chassis. Reference (black) and equivalent (red for surface, blue for volumetric and green for ad hoc equivalent source distribution) values are reported

TABLE 5 Model prediction—Scenario Figure 9

Eq. sourcesplacement	D_{ref}(dBi)	D_{eq}(dBi)	E_{eq}/E_{ref}(dB)	D_{est}(dBi)
Volumetric	6.7	5.2	0.08	4.5
Surface	6.7	5.0	0.99	4.5
Ad hoc	6.7	6.6	0.02	4.5

Figure 10 and Table 5 show that the 'ad hoc' choice leads to better results, in addition to a reduction of computational resources.

As regards the prediction of the maximum value of the radiated electric field, the three choices of the equivalent source positioning provide similar results with a good level of accuracy. However, the 'ad hoc' positioning of the equivalent sources, deduced by a physical inspection of the EUT and resulting from an *a priori* electromagnetic analysis, returns not only a good accuracy of the radiated field but also a good reconstruction of the emission pattern of the EUT.

These results confirm that the method is more accurate and efficient, the more we are able to enter information on the physical behaviour of the field source.

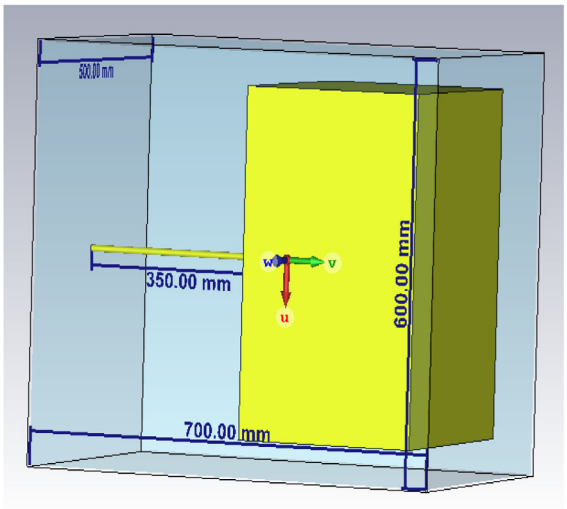

FIGURE 11 The EUT: A metallic box with a cable

TABLE 6 Radiated emission—Scenario Figure 11

Eq. sourcesplacement	D_{ref}(dBi)	D_{eq}(dBi)	E_{eq}/E_{ref}[dB]	D_{est}(dBi)
Volumetric	4.8	5.1	1.06	4.9
Surface	4.8	4.9	−0.90	4.9
Ad hoc	4.8	4.9	−0.22	4.9

4.3 | EUT with a cable protruding from a metallic chassis

The last analyzed scenario is another typical situation arising in an EMC context. We now consider an EUT having a cable of 35 cm protruding from a metallic chassis (Figure 11). In a realistic context the cable can be the metallic support of a noise current, giving rise to a common mode radiation. Therefore, in this case, after a visual inspection, the cable can be identified as an emission source. As in the other examples, the simple geometry allows us to analytically evaluate the reference field radiated by a current flowing along the cable [29].

Simulations are carried out at 1 GHz with a grid step of 5 cm, and comparing three equivalent source distributions:

- volumetric, choosing the largest possible ESV for the considered RC (70 cm × 60 cm × 50 cm), so as to include the cable and its image; in this scenario, 2145 grid points are considered;
- superficial, choosing only the subset of the equivalent sources corresponding the EUT's external surface; in this scenario, 858 grid points are considered;
- 'ad hoc', choosing only the subset of the equivalent sources corresponding to the cable. In this configuration, only 15 equivalent sources are used (only the electric dipoles directed along the direction of the cable).

Figure 12 and Table 6 also show that in this scenario the 'ad hoc' placement of the equivalent sources leads to the most reliable reconstruction of the emission pattern and the prediction of the maximum electric field radiated in free space.

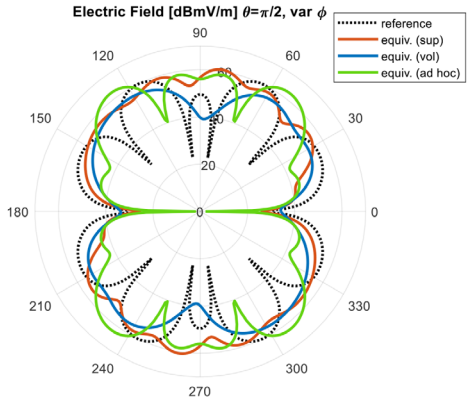

FIGURE 12 Electric field at the distance of 10 m radiated by a EUT having a 35 cm cable protruding from a metallic chassis. Reference (black) and equivalent (red for surface, blue for volumetric and green for ad hoc equivalent source distribution) values are reported

We can see that when many grating lobes are present, the reconstruction of the emission pattern is more critical, even if it can be improved using ad hoc equivalent sources. Nevertheless, the maximum radiated field value is well predicted, as in the previous cases.

5 | CONCLUSIONS

The work deals with the prediction of the radiated emissions of an EUT in free space from the knowledge of field samples collected on the RC's walls. Under the assumption that the power radiated in free space and in the chamber are quite similar, as in a well-stirred RC, the proposed method consists of replacing the EUT with a set of equivalent sources able to reproduce the same field within the RC.

The equivalent sources thus determined produce a free space radiated field which is a good approximation of the one effectively radiated by the EUT.

The results obtained for various practical situations show different levels of approximation, but the agreement is always quite satisfactory, with a maximum difference of less than 2 dB in the worst case.

Results are improved if we can add some *a priori* information about the EUT's electromagnetic nature and its geometry. This means that the method is very flexible, because if we have *a priori* knowledge of the dominant unintentional source characteristics, the choice of the corresponding subset of equivalent sources is more effective and results are more accurate both for maximum field strength and emission pattern.

The method, tailored for an MMSS RC, has three main advantages: for an emission test, no additional hardware is required inside the chamber other than that required for an immunity test; the value of the radiated emission in all directions is directly obtained without the need for preliminary computation of the total radiated power; nothing is moved within the chamber.

These preliminary results are very encouraging and suggest continuing the analysis in order to investigate the robustness of the method and its accuracy when field samples of only the modulus are used. This alternative formulation of the method would be useful in standard emission measurements, where only the amplitude of the electric field is measured using a spectrum analyzer or an EMI receiver. The effect of uncertainty in field sample positions on the accuracy of the reconstructed field will also be analyzed for a future applicability of the proposed method in experimental measurements.

REFERENCES

1. Corona, P., et al.: Use of a reverberating enclosure for measurements of radiated power in the microwave range. IEEE Trans. Electromagn. Compat. EMC-18(2), 54–59 (1976)
2. Serra, R. et al.: Reverberation chambers a la carte: An overview of the different mode-stirring techniques. IEEE Electromagn. Compat. Mag. 6(1), 63–78 (2017)
3. Besnier, P., Démoulin, B.: Electromagnetic Reverberation Chambers. Wiley-ISTE, Hoboken (2013)
4. Reverberation chamber test methods, International Electrotechnical Commission (IEC), Std. 61 000-4-21, (2011)
5. Candidi, M., et al.: Comparison of radiated emission measurements for 500 MHz to 2GHz in various EMC Facilities. In: Proceedings of EMC Europe 2002: International Symposium on Electromagnetic Compatibility, Sorrento (2002)
6. Koepke, G., et al.: Directivity of the test device in EMC measurements. In: Proceedings of 2000 IEEE International Symposium on EMC, Washington, DC (2000)
7. Lemoine, C., et al.: Antenna directivity measurement in reverberation chamber from Rician K-factor estimation. IEEE Trans. Antennas Propag. 61(10), 5307–5310 (2013)
8. García-Fernández, M.Á., et al.: Antenna gain and radiation pattern measurements in reverberation chamber using doppler effect. IEEE Trans. Antennas Propag. 62(10), 5389–5394 (2014)
9. Fiumara, V., et al.: Free-space antenna pattern retrieval in nonideal reverberation chambers. IEEE Trans. Electromagn. Compat. 58(3), 673–677 (2016)
10. Leferink, F.B.J., et al.: OATS emission data compared with free space emission data. In: Proceedings of International Symposium on Electromagnetic Compatibility, Atlanta (1995)
11. Sreenivasiah, I., Chang, D.C., Ma, M.T.: Emission of electrically small radiating sources from tests inside a TEM Cell. 1979 IEEE International Symposium on Electromagnetic Compatibility, San Diego (1979)
12. Wilson, P.: On correlating TEM cell and OATS emission measurements. IEEE Trans. Electromagn. Compat. 37(1), 1–16 (1995)
13. Wilson, P., Holloway, C.L., Koepke, G.: A review of dipole models for correlating emission measurements made at various EMC test facilities. In: International Symposium on Electromagnetic Compatibility, Silicon Valley (2004)
14. Turnbull, L., Marvin, A.C.: A treatment of the phase properties of GTEM to open-area test-site correlation techniques. IEEE Trans. Electromagn. Compat. 40(1), 62–69 (1998).
15. Heidemann, M., Garbe, H.: Improvement of GTEM to OATS correlation. In: IEEE International Symposium on Electromagnetic Compatibility. Symposium Record (Cat. No. 00CH37016), Washington, DC (2000)
16. Ngu, X.T.I., et al.: A complete model for simulating magnitude and phase of emissions from an EUT placed inside a GTEM cell. IEEE Trans. Electromagn. Compat. 49(2), 285–293, (2007)
17. Garbe, H., Battermann, S.: Converting total-radiated-power measurements to equivalent E-field data. In: IEEE International Symposium on Electromagnetic Compatibility, Detroit (2008)
18. Gerth, H., et al.: New advances on correlating TEM cell and OATS emission measurements. IEEE Trans. Electromagn. Compat. 52(1), 11–20 (2010)
19. CISPR 16-4-5. Conditions for the use of alternative test methods (2006)
20. Krauthauser, H.G.: Statistical analysis of the correlation of emission limits for established and alternative test sites. IEEE Trans. Electromagn. Compat. 53(4), 863–875 (2011)
21. De Leo, A., et al.: Low-frequency theoretical analysis of a source-stirred reverberation chamber. IEEE Trans. Electromagn. Compat. 59(2), 315–324 (2017)
22. Leo, A.D., et al.: Experimental validation of an analytical model for the design of source-stirred chambers. IEEE Trans. Electromagn. Compat. 60(2), 540–543 (2018)
23. Hill, D.A.: Spatial correlation function for fields in a reverberation chamber. IEEE Trans. Electromagn. Compat. 37(1), 138 (1995)
24. De Leo, A., et al.: Numerical analysis of a reverberation chamber: Comparison between mechanical and source stirring techniques. In: 2017 International Symposium on Electromagnetic Compatibility - EMC EUROPE, Angers (2017)
25. De Leo, A., et al.: Well-stirred condition method applied to a multiple monopole source stirred reverberation chamber. In: 2020 International Symposium on Electromagnetic Compatibility - EMC EUROPE, Rome (2020)
26. De Leo, A., et al.: Experimental comparison between source stirring and mechanical stirring in a reverberation chamber by analyzing the antenna transmission coefficient. In: 2018 International Symposium on Electromagnetic Compatibility (EMC EUROPE), Amsterdam, (2018)
27. Van Bladel, J.G.: Electromagnetic Fields. IEEE Press Series on Electromagnetic Wave Theory, pp. 509–562.Wiley, Hoboken. (2007)
28. De Leo, A., et al.: A novel emission test method for multiple monopole source stirred reverberation chambers. IEEE Trans. Electromagn. Compat. 62(5), 2334–2337 (2020)
29. De Leo, A., et al.: Analytical prediction of common mode noise in a source stirred reverberation chamber. In: IEEE International Symposium on Electromagnetic Compatibility (EMC), Dresden (2015)

How to cite this article: De Leo A, Cerri G, Russo P, Mariani Primiani V. A general method for radiated emission prediction in a multiple monopole source stirred reverberation chamber. IET Sci Meas Technol. 2021;15:588–596. https://doi.org/10.1049/smt2.12060